Applied Thermal Engineering 126 (2017) 1115–1125

Contents lists available at ScienceDirect

Applied Thermal Engineering

journal homepage: www.elsevier.com/locate/apthermeng

Research Paper

Startup characteristics of pump-assisted capillary phase change loop

Chi Jiang, Wei Liu *, Zhichun Liu, Jinguo Yang, Bin Duan, Xiaobing Luo

School of Energy and Power Engineering, Huazhong University of Science and Technology, Wuhan 430074, PR China

HIGHLIGHTS

- A self-designed impeller pump was used in the pump-assisted capillary loop.
- The pre-conditions on the startup characteristics were classified and analyzed.
- The pump-assisted capillary loop was validated to handle well with bubble generated in CC.

ARTICLE INFO

Article history:
Received 7 September 2016
Revised 11 January 2017
Accepted 11 February 2017
Available online 14 February 2017

Keywords:
Startup
Impeller pump
Pre-conditions
Temperature overshoot
Heat leak

ABSTRACT

In this study, startup characteristics of a pump-assisted capillary phase change loop under various operational conditions were experimentally investigated. For the loop fabrication, a self-designed impeller pump was selected to reduce the volume and weight of the loop. Methanol was chosen as the working fluid. The test results indicated that the pre-conditions in the evaporator had a large impact on the startup characteristics. When the vapor chamber was occupied, partially or completely, with liquid before startup, a temperature overshoot appeared in the heater wall temperature profile. As a higher heat load was applied to the evaporator, vapor bubbles generated in the compensation chamber. Under these conditions, the loop still operated steadily, and the heat transfer capability of the evaporator improved. To avoid the boiling conditions that appeared in the compensation chamber, either lowering the heat sink temperature or increasing the pumping power was the effective manner.

1. Introduction

As the heat flux of electronic components gradually increases, a highly efficient cooling system is required. Among the numerous cooling technologies, heat transfer via phase change of the working fluid is considered as an efficient method. Previously, the capillary-driven loops, such as capillary pumped loops (CPLs) and loop heat pipes (LHPs), which served as a typical two-phase loop, were used to dissipate the high heat flux [1–5]. The operation of the loops relies on the capillary force generated in the evaporator without external power consumption [6–9]. Meanwhile, based on the shape of the evaporator, LHPs can be divided into the two types: cylindrical and flat-plate. In contrast to the cylindrical evaporator, the flat-type evaporator directly contacts the heater surface, which vastly decreases the thermal resistance between the heater wall and the evaporator. The flat-type LHP possesses a high heat transfer efficiency. However, as the miniaturization of the flat-type LHP, the capillary pressure head the evaporator developed decreases, which restricts the loop performance, such as the effective length of the loop and the maximum heat load applied to the evaporator [10–12]. Moreover, owing to the structure of the flat evaporator, the heat is likely to leak from the evaporator to the compensation chamber, leading to a change in the thermal and hydrodynamic conditions in the compensation chamber. This causes temperature oscillation in LHP [13–15]. Therefore, to overcome the shortcomings in LHP, a pump-assisted capillary phase change loop was proposed [16]. As shown in Fig. 1, pump-assisted capillary phase change loop consisted of an evaporator, a condenser, an ejector, a reservoir, a mechanical pump, and transport lines. During operation of the loop, liquid in the reservoir was forced by the pump through the evaporator. In the evaporator, the liquid was divided into two separated branches. Most of the liquid flowed through the compensation chamber, while only a small amount of liquid passed through the porous wick to vapor chamber. The liquid in the vapor chamber absorbed heat and then evaporated. Subsequently, the generated vapor flowed through the vapor channels to the vapor line and was cooled in condenser #1. Meanwhile, a small quantity of heat, called heat leakage, transferred through the evaporator sidewall to the compensation chamber. The heat leak was removed by the flowing liquid through the compensation chamber. The heated liquid passed through the compensation

* Corresponding author.
E-mail address: w_liu@hust.edu.cn (W. Liu).

http://dx.doi.org/10.1016/j.applthermaleng.2017.02.043
1359-4311/

Nomenclature

P	pumping power, W
Q	heat load, W
T	temperature, °C

Subscripts

sink	heat sink

Abbreviations

Amb	ambient temperature, °C
CC	compensation chamber
CC-in	compensation chamber inlet temperature, TC15
CC-out	compensation chamber outlet temperature, TC6
Cond-#1-in	condenser #1 inlet temperature, TC8
Cond-#2-in	condenser #2 inlet temperature, TC7
Evap-out	evaporator outlet temperature, TC5
wall	heater wall temperature, average of TC1-TC4

chamber outlet and reached condenser #2. In the condenser, vapor and the heated liquid released heat and transformed to the subcooled state. The subcooled liquid at the condenser outlets was combined in the ejector and then forced back to the reservoir. With the assistance of the pump, the liquid began to circulate for the next circle. Based on the running process of the pump-assisted capillary phase change loop, the liquid transmission capability increased by adding a pump in the loop. The loop could meet the requirement of transport distance by properly adjusting the power consumption of the pump. Meanwhile, in the evaporator, latent heat of the working fluid was used to dissipate heat. For the same heat flux, utilizing phase change required less circulating working fluid than the single-phase loop. As a combination of active cooling and passive cooling loop, pump-assisted capillary phase change loop possessed high heat transfer capability, long transport distance, and strong operational stabilization.

Until recently, a number of experimental investigations on pump-assisted capillary loop have been performed. Specifically, Park et al. [17–19] performed a series of experiments on pump-assisted capillary phase change loop. In the experimental study, the effect of external conditions on the operational characteristics of the loop was tested in detail. The results indicated that the loop had the potential to dissipate high heat flux. No obvious temperature oscillation was found throughout the loop. Babin et al. [20] proposed an analytical model to predict the performance of the pump-assisted capillary loop. The results of the analytical model revealed an increase in performance ranging from 20% to 100% owing to the addition of an ion-drag pump. Simultaneously, an experimental loop was developed to verify the accuracy of the analytical model. Schweizer et al. [21] designed a mechanically pumped two-phase loop by inserting an annular gear pump into the liquid line to provide the mechanical pumping force. The test results showed that the loop worked adequately in all orientations. Hoang et al. [22] proposed a mechanical/capillary hybrid pump loop and selected the ABI bearingless pump as the mechanical pumping force. A three-month performance test was performed on the test loop to establish the operational characteristics. The test results indicated that the loop could run smoothly during the entire operating periods. The loop in this study was quite different from other studies. In Park's loop [17–19], the evaporator contained a complex structure and was coupled with the heater block. This was not practical for cooling an actual electronic device. Meanwhile, the reservoir not only contained the excess liquid in the loop but also played a role to cool the vapor from the vapor line. This created a complex loop structure and was not suitable for a compact design of the loop. In Babin's work [20], only the prototype of the loop was proposed. The author chose the ion-drag pump to provide the pumping force, which led to a complex pump control system. Moreover, for selection of the working fluid, the polarity of the working fluid should be considered, which would restrict the selection range of the working fluid. For the loop presented by Schweizer [21], no excess liquid outlet was designed on the compensation chamber. Therefore, the pumping liquid would entirely pass through the porous wick. This would lead to an increase of flow resistance of the loop. In addition, the generated vapor in the vapor chamber would be eliminated by the pumping liquid, and then, the evaporator would operate with low heat transfer efficiency. In Hoang's work [22], the cylindrical evaporator increased the thermal contact resistance. This led to the degradation of the evaporator performance. In this study, efforts were made to improve the loop performance. To decrease the evaporator size and the thermal contact resistance, the evaporator was designed in flat type, which could easily contact the heat source. To reduce the flow resistance of loop, excess liquid outlet was designed on the compensation chamber. Meanwhile, the placement of the porous wick in the evaporator effectively sepa-

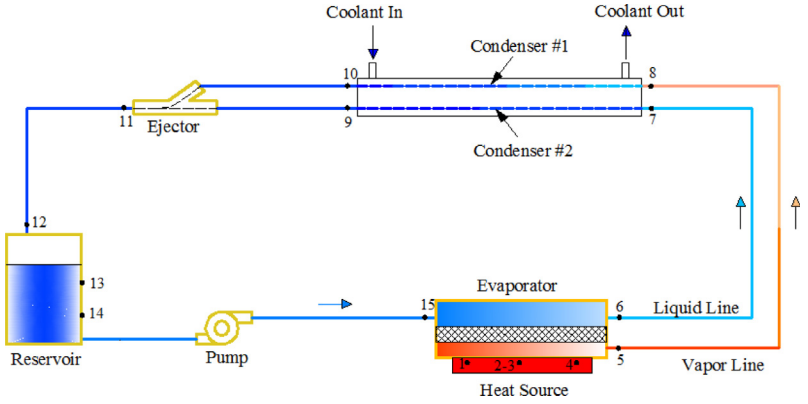

Fig. 1. Schematic of the pump-assisted capillary loop and the main test points throughout the loop.

rated the liquid flow in the compensation chamber and vapor flow in the vapor chamber from penetrating. Therefore, a large pressure drop and the corresponding pumping power due to the two-phase mixture flow were prevented.

As discussed above, most of the previous studies remained in the prototype stage that only the reliability of the pump-assisted capillary phase change loop was evaluated. However, the operational mechanism was not extensively considered. The situation of startup always encounters for the actual application of a cooling system. For a two-phase loop, variations of input operational condition before startup have a profound impact on the operational characteristics of the loop. In study of two-phase fluid loop and LHP, situations associated with startup have been extensively investigated and analyzed [23–29]. Liu et al. [23] observed a superheating phenomenon in the evaporator during startup. The superheat was confirmed to correlate to the evaporating temperature and the initial liquid distribution in the evaporator. Similar phenomena were encountered during the startup process of an LHP [24–29]. It was concluded that different liquid-vapor distributions in the evaporator resulted in a diverse heat and mass transfer processes, and then led to different startup time or diverse temperature overshoots. Different startup characteristics from different liquid-vapor distributions in an LHP made the operational temperature unpredictable. Nevertheless, the research conclusions could be adopted to weaken the influence of initial liquid-vapor distribution and to avoid the overlarge temperature overshoot.

One of the main idea for designing a pump-assisted capillary phase change loop is to solve the problem of startup failure. Moreover, the startup process is an important criterion for evaluating the heat response and heat transfer ability of a cooling system. However, the startup characteristic of the pump-assisted capillary loop has not been revealed yet. Therefore, studying startup characteristics of the loop is significant to verify the effectiveness of the design. In this study, a new pump-assisted capillary phase change loop was designed, and a self-designed impeller pump was selected to provide the pumping force. We expected to obtain a comprehensive understanding of the startup characteristics of the loop. The findings regarding the operational mechanism of the startup process of the present design may provide practical guidelines for application of the loop in high power density electronic devices or in future space applications.

2. Experimental setup

A typical pump-assisted capillary phase change loop consists of an evaporator, a condenser, an ejector, a mechanical pump, a reservoir, liquid, and vapor transport lines. Fig. 2 shows the system diagram of the loop. In this study, the loop was made of stainless steel except for the evaporator and the condenser. The evaporator was made of brass and designed in a flat disk shape. The evaporator structure is shown in Fig. 3. On the sidewall of the evaporator, three round holes were designed, for the compensation chamber inlet, the compensation chamber outlet, and the evaporator outlet. In the practical design, the direction of the evaporator outlet was vertical to the compensation chamber inlet and outlet. Figs. 3 (a) and (b) show the sectional views of the evaporator in different orientations. To depict the status of the working fluid at the three evaporator outlets in the same dimension, the evaporator outlet and right portion of the vapor chamber were rotated from the vertical orientation to a parallel orientation in Fig. 3(c). The thickness of the evaporator wall was 1.5 mm. In this study, the impeller pump, which was designed and fabricated autonomously to reduce the weight of the loop, was selected to provide the mechanical pumping force [30]. The entity of the pump is shown in Fig. 4, and the weight of the pump was less than 150 g. A pipe-in-pipe heat exchanger was chosen as the condenser. In order to enhance the heat exchange between the working fluid and the cooling water, a pure copper tube was selected as the inner one. Detailed parameters of the loop are summarized in Table 1.

In this study, methanol with a purity of 99.5% was chosen as the working fluid. Before liquid charged into the loop, the loop was evacuated. In our previous work [31], the impact of two different liquid charging methods on the operational characteristics of pump-assisted capillary phase change loop was extensively investigated. It was found that degassing the charging system and the loop as a whole, and then filling the determined working fluid were a superior method to decrease the leakage of non-condensable gas into the loop. Therefore, this superior liquid charging method was adopted in this study. Specifically, a sealed charging system was connected to the loop. The entire system was then vacuumized to a pressure of 3.2×10^{-4} Pa. Subsequently, predetermined working fluid was charged into the loop through the charging system. In this study, the charging ratio was selected as 75%. During all of the test periods, a vacuum condition was maintained in the loop.

In the experiment, the heat load applied to the evaporator was provided by a copper heat block with several imbedded cartridge heaters. The active heater area of the heat block was 10.2 cm^2. The variable heat load was measured by a wattmeter with an accuracy of 0.5%. T-type thermocouples were selected to monitor the temperature throughout the loop. The placement of the main measure points is labeled in Fig. 1. The accuracy of the thermocouple was ±0.5 °C. Non-condensable gases in pump-assisted capillary loop would increase the vaporization temperature of the loop, leading to the degradation of loop performance. Since adding the flowmeter in the loop may bring in leakage point, the flowmeter was not considered in the loop design. Instead, measuring power consumption of the pump is used for evaluating the variation of

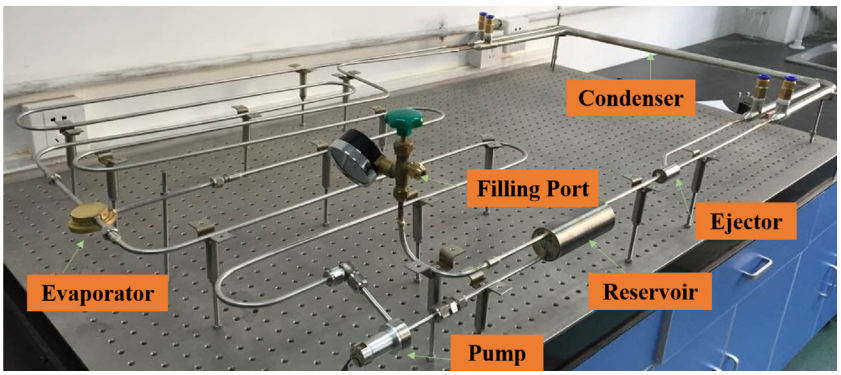

Fig. 2. System diagram of pump-assisted capillary phase change loop.

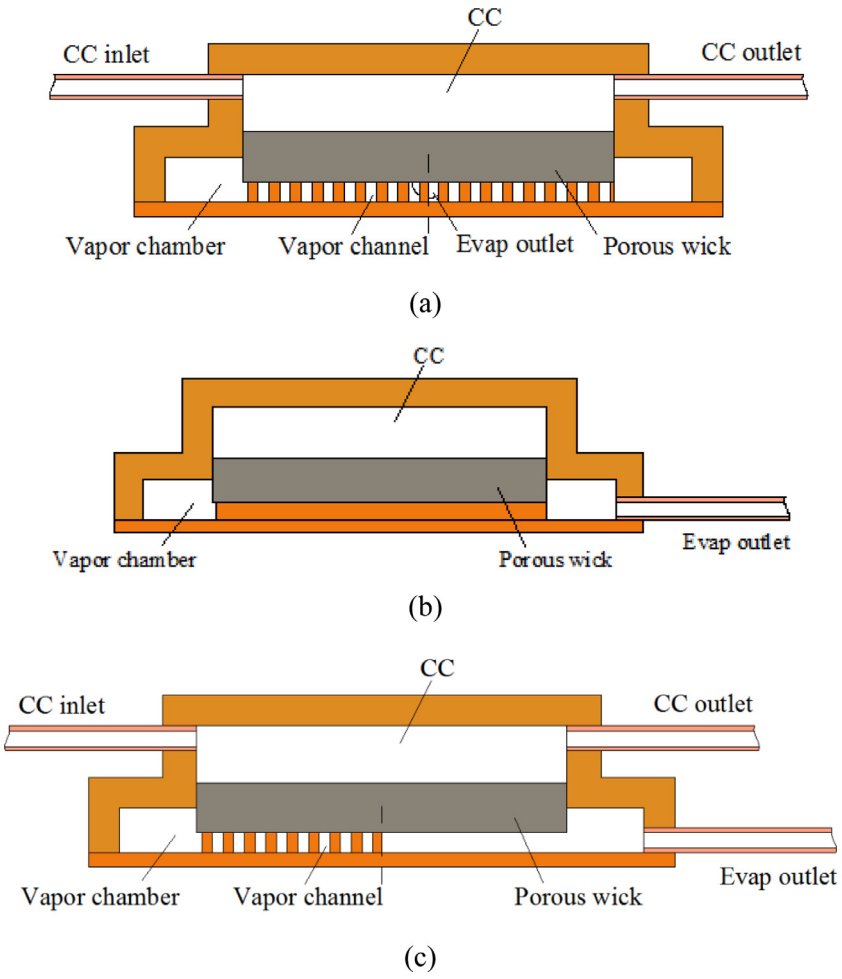

Fig. 3. Schematic of the evaporator: (a) & (b) Sectional views of evaporator in different orientations, (c) the rotated sectional view of evaporator.

Fig. 4. Entity of the impeller pump.

liquid flow rate. Then, a digital power meter with accuracy of 0.2% was connected to monitor the power consumption of the pump. During the test period, the air temperature was between 17 °C and 26 °C.

3. Results and analysis

The experimental results depict the startup characteristics of the loop under different operational conditions. Before each test, the chilling unit produced cooling water at the expected temperature. The cooling water was forced into the interlayer of the condenser tube, to cool the working fluid in the condenser. Then, a mechanical pump started and circulated the working fluid in the loop. When the loop reached a cold equilibrium, the heat load was applied to the evaporator. Subsequently, the thermocouples recorded the temperature variation throughout the loop. When no obvious temperature variation was found at the prescribed heat load, the startup process of the loop was completed.

3.1. Effect of the heat load

Previous works revealed that the pump-assisted capillary phase change loop exhibited different characteristics of wick flooding and thin-film boiling, depending on the pressure difference between the vapor chamber and the compensation chamber [16,31]. Since the liquid pressure in the compensation chamber was directly determined by the pressure head of the mechanical pump, with a constant pumping power, the pressure difference was related to the vapor pressure in the vapor chamber. When heat loads applied to the evaporator were altered, the generated vapor pressure changed. Subsequently, the loop exhibited diverse startup characteristics.

As heat load was applied to the evaporator, the heat flux spread to the porous wick, causing liquid evaporation on the wick surface. The vapor generated and gathered in the vapor chamber. When a low heat load was applied, as shown in Fig. 5(a), the vapor pressure was lower than the liquid pressure in the compensation chamber. Therefore, the vapor was eliminated by the liquid owing to the

Table 1
Main parameters of the pump-assisted capillary loop.

Components		Dimensions
Evaporator		
	Heated diameter	46.0 mm
	Total height	17.0 mm
	CC diameter	37.8 mm
	CC height	9.8 mm
	Material	Brass
Porous wick		
	Diameter	37.4 mm
	Thickness	3.2 mm
	Porosity	69.0%
	Material	Nickel
Vapor line		
	Diameter I/O	4.0/6.0 mm
	Length	2340.0 mm
	Material	Stainless steel
Liquid lines		
	Diameter I/O	4.0/6.0 mm
	Length	4590.0 mm
	Material	Stainless steel
Pipe-in-pipe Condenser		
	Inner tube diameter I/O	4.0/6.0 mm
	Outer tube diameter I/O	14.0/16.0 mm
	Length #1/#2	1360.0/1440.0 mm
	Inner tube material	Pure copper
Reservoir		
	Inner volume	96.7 ml
	Material	Stainless steel
Charging ratio		
		75.0%

pressure difference, and, only the liquid sensible heat was used to transfer heat. The evaporator was entirely occupied with liquid. Liquid flowed through the evaporator outlet and then reached condenser #1. Since the liquid temperature was lower than the ambient temperature, liquid flowed slowly through the vapor line and absorbed heat from the ambient environment. Owing to the back-heat conduction at the condenser #1 inlet, liquid released the sensible heat. Therefore, as presented in the startup profile in Fig. 5(a), the liquid temperature at the condenser #1 inlet was slightly larger than that at the evaporator outlet. This situation corresponded to the wick-flooding mode. As the applied heat load increased, as shown in Fig. 5(b), the generated vapor pressure increased and became larger than the liquid pressure in the compensation chamber. Then, stable vapor occupied the vapor chamber and wick flooding was replaced by thin-film boiling in the evaporator. The vapor took away the heat and flowed rapidly to condenser #1. As vapor reached condenser #1, a remarkable temperature increase appeared at the condenser #1 inlet, as shown in the startup profile in Fig. 5(b). Meanwhile, when the evaporator reached stabilization, the temperature at the evaporator outlet and the condenser #1 inlet remained nearly uniform. As the heat load continued to increase, as shown in Fig. 5(c), the vapor in the vapor chamber gradually transformed to a superheated state. The operational mode entered the vapor-superheating mode. As shown in the startup profile in Fig. 5(c), a similar temperature increase of the condenser #1 inlet temperature occurred as the vapor reached condenser #1. Converse to the thin film-boiling mode, when the thermal equilibrium reached at the superheating mode, the evaporator outlet temperature was greater than the condenser #1 inlet temperature. Therefore, according to the profile trend of the evaporator outlet and the condenser #1 inlet, we classified the startup characteristics into three different operational modes.

The three startup modes in this study contained an identical law shown in our previous work [31]. Therefore, the three startup modes of wick flooding, thin-film boiling, and vapor superheating represented typical operational modes for the pump-assisted capillary phase change loop.

With the use of a pump in the pump-assisted capillary phase change loop, several startup characteristics were different from that in an LHP. First, when using a pump, the startup capability of pump-assisted capillary loop under a low heat load was improved. The loop could successfully start up even though a low heat load was applied to the evaporator. Second, altering the input operating conditions of the pump-assisted capillary loop during the startup redistributed the working fluid in the evaporator. Since liquid pressure in the compensation chamber is a direct function of the pumping power, varying the pumping power led to different pressure relationships between the vapor pressure in the vapor chamber and the liquid pressure in the compensation chamber. When the liquid pressure was larger than the vapor pressure, the vapor phase vanished and the evaporator was entirely occupied with liquid. The applied heat load to the evaporator was dissipated by the liquid sensible heat. Conversely, when the vapor pressure was larger than the liquid pressure, a stable liquid-vapor interface was formed in the porous wick. The applied heat load to the evaporator was dissipated by the latent heat of the working fluid. According to different input conditions, the pump-assisted capillary loop could automatically shift the operating mode to satisfy the heat dissipation demand. However, in an LHP operation, the vapor pressure was always larger than the liquid pressure. The successful startup of an LHP signified the vapor phase circulated in the loop. Differing from pump-assisted capillary phase change loop, LHP could not shift the operating condition to transport heat. Only if the stable vapor phase formed in the evaporator could the LHP successfully start up. Third, for a flat-type evaporator, heat easily leaked from the vapor chamber to the compensation chamber. In an LHP operation under certain operational conditions, the heat leak would cause nucleate boiling in the compensation chamber. Then, the generated vapor in the compensation chamber would block the liquid supply to the porous wick. This would result in startup failure or operating temperature oscillation. However, with the use of a pump in pump-assisted capillary loop, the heat leak was removed by liquid convection in the compensation chamber. Liquid supply for evaporation was guaranteed by the forced pumping liquid. Therefore, the robustness of the loop was strengthened owing to the addition of a pump. In summary, with the use of a pump, pump-assisted capillary phase change loop could achieve the startup stabilization and the flexibility of startup mode.

3.2. Effect of initial liquid-vapor distribution in the evaporator

Fig. 6 shows the variations of the evaporator outlet temperature and the condenser #1 inlet temperature against the heat load under different operational conditions. The temperature points on the figure were obtained at the steady state. Presenting both the evaporator outlet and the condenser #1 inlet in the figure was to distinguish the three different modes. For the test points in the loop, the evaporator outlet temperature was considered approximately equal to the temperature of the working fluid in the vapor chamber. That meant the evaporator outlet temperature corresponded to the evaporation temperature, when the thin film boiling mode took place in the evaporator. As shown in Fig. 6, when the evaporator operated in the thin-film boiling mode (no obvious temperature difference was found between the evaporator outlet and the condenser #1 inlet, e.g. a heat load ranging from 20 W to 70 W with pumping power of 2 W at a heat sink temperature of 10 °C), the evaporator outlet temperature remained nearly constant. In other words, the evaporation temperature stayed the same regardless of the variation of the heat load. Moreover, the evaporation temperature varied along with the variation of heat

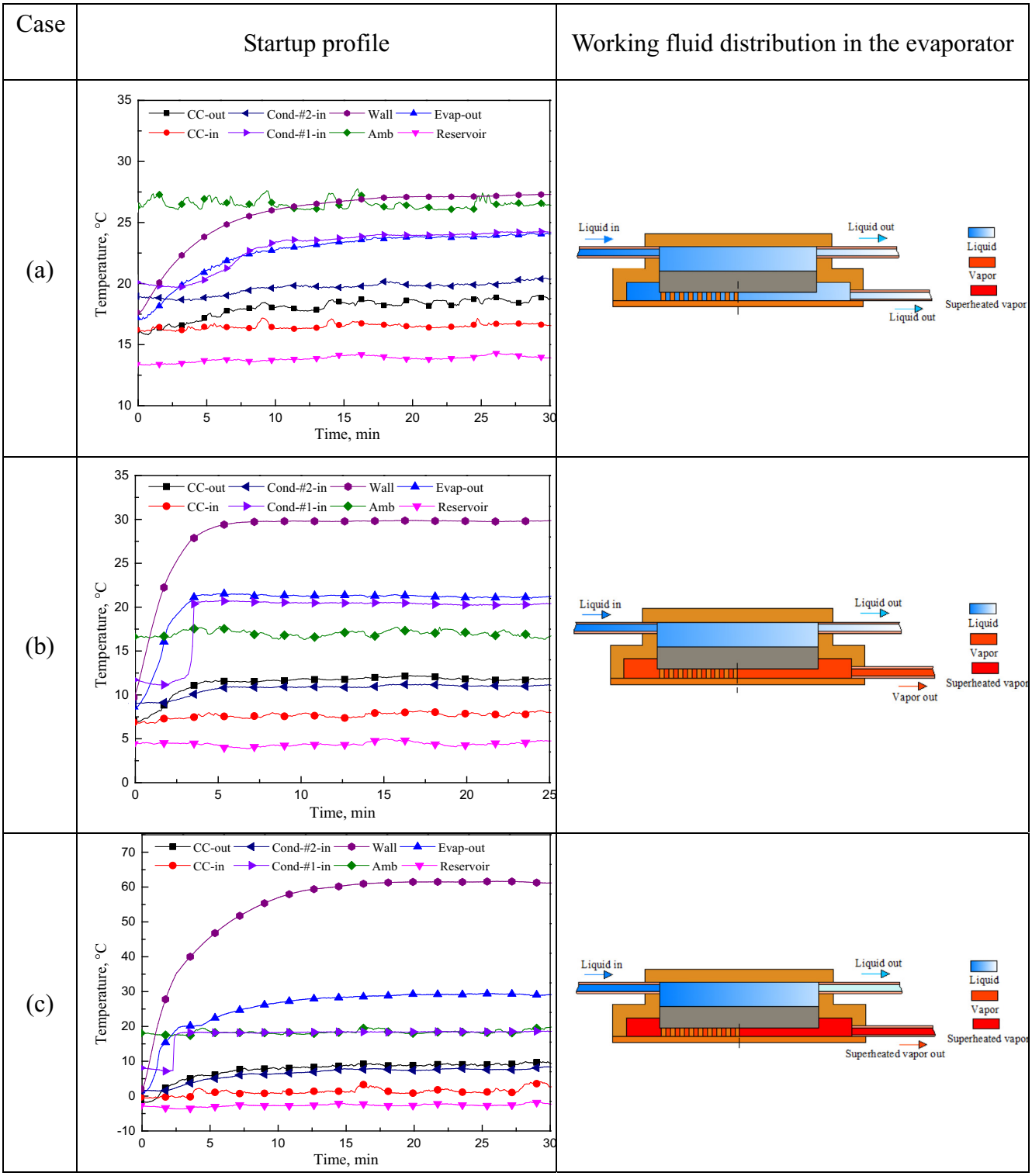

Fig. 5. Startup characteristics of the loop and status of working fluid in the evaporator under different heat loads: (a) $Q = 10$ W, $P = 1.8$ W, $T_{sink} = 10$ °C, (b) $Q = 40$ W, $P = 1.8$ W, $T_{sink} = 0$ °C, (c) $Q = 90$ W, $P = 1.8$ W, $T_{sink} = -10$ °C.

sink temperature. For the pumping power of 2 W and, as the heat sink temperature dropped from 10 °C to −10 °C, the evaporation temperature varied from 25 °C to 17 °C. Meanwhile, changing the pumping power had nearly no impact on the evaporation temperature. For the heat sink temperature of 0 °C, as the pumping power changes from 1.8 W to 2 W, the evaporation temperature remained at the temperature level of 21.5 °C. Therefore, the evaporation temperature was known for the given heat sink temperature. In addition, the evaporation temperature was simply influenced by the heat sink temperature instead of the pumping power and the heat load.

3.2.1. Different startup characteristics

In the experiments, the loop was placed in the horizontal plane. Thus, the evaporator and the condenser were at the same height. Fig. 7 shows the startup characteristics of the loop under different

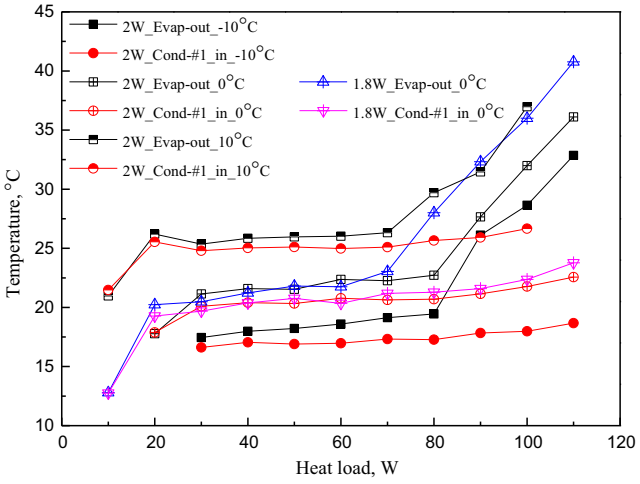

Fig. 6. The variations of evaporator outlet temperature and condenser #1 inlet temperature against heat load under different operational conditions.

operational conditions. As shown in the figures, the startup characteristics under different operational conditions showed similar trends. The temperature overshoot of the heater wall all appeared during the startup processes.

After the heat load was applied to the evaporator, as illustrated in Fig. 7(a), the heater wall temperature and evaporator outlet temperature raised immediately. The working fluid in the vapor chamber absorbed heat and flowed to the condenser. The condenser #1 inlet temperature followed the trend of the evaporator outlet. At a startup time between 15 min and 20 min, the loop reached equilibrium with no obvious temperature variation. Despite the evaporator outlet temperature exceeding 21.5 °C, which means the evaporation temperature of the working fluid at the heat sink temperature of 0 °C was reached, no vapor generated in the vapor chamber. This was determined by observing the temperature difference between the evaporator outlet and the condenser #1 inlet. At this condition, the liquid in the vapor chamber gradually transferred to the superheated state, which was not a stable state. Subsequently, the superheated liquid continued to absorb heat. When the metastable state was broken, the superheated liquid transformed to vapor. Then, the heat transfer performance of the evaporator naturally contained a prominent enhancement. Therefore, a sharp temperature drop appeared on the heater wall. Meanwhile, owing to the arrival of the vapor to the condenser #1, the evaporator outlet temperature and the condenser #1 inlet temperature rapidly varied to be uniform, and then the loop reached the stable state. A similar state change of the working fluid in the evaporator and the variation of the temperature profiles are shown in Figs. 7(b) and (c).

During the above three operational conditions, the evaporator was first in an unstable state, and then reached an equilibrium state as the vapor was generated in the vapor chamber. The remaining startup characteristics presented in Figs. 7(d)–(f) differed from that mentioned above in Fig. 7(a)–(c), although a uniform temperature overshoot occurred. As illustrated in Fig. 7(d), the temperature at each test point increased, after the heat load was applied to the evaporator. When the evaporator outlet temperature reached 25 °C, which means the evaporation temperature of the working fluid at the heat sink temperature of 10 °C is reached, the step increase of the condenser #1 inlet temperature occurred. Therefore, thin-film boiling occurred in the evaporator, and then vapor occupies the entire vapor chamber. Afterwards, the loop appeared to reach a stable state, with vapor moving smoothly to the condenser. However, with a start time of 8.5 min, a slight spike of the evaporator outlet temperature appeared. Then, a notable temperature drop occurred on the heater wall. This could be because of the heat transfer enhancement in the evaporator, indicating that slightly more vapor was generated in the vapor chamber. Because of this regenerated vapor, a slight spike of temperature appeared at the condenser #1 inlet as well. In Figs. 7(e) and (f), similar operational conditions were concluded even though there was not a spike observed at the evaporator outlet. The similarity in Figs. 7(d)–(f) appeared that a temperature drop on the heater wall occurred after the vapor was generated in the vapor chamber. The main reason for the different startup characteristics shown in Fig. 7 is analyzed in the next section.

3.2.2. Analysis

The experimental results presented in Fig. 7 indicated that the internal conditions in the evaporator were likely to influence the startup behavior of the loop. Before the heat load was applied to the evaporator in Figs. 7(a)–(c), the loop was shut down for one night. The working fluid in the loop was redistributed after the shutdown. Since the vapor chamber was placed lower than the compensation chamber, condensed liquid was generated in the vapor chamber. Meanwhile, the gap between the evaporator inner wall and the wick helped the liquid leaking from the compensation chamber to the vapor chamber. Therefore, the vapor chamber was fully occupied with liquid before startup. When the heat load was applied, owing to no effective nucleation sites existing in the vapor chamber, the liquid in the vapor chamber did not vaporize even though the liquid exceeded the evaporation temperature. Hence, the liquid in the vapor chamber was in a superheated state. The utilization of single-phase heat transfer led to a higher heater wall temperature. As the superheat degree of the liquid gradually increased, the metastable equilibrium in the evaporator became unstable. Subsequently, the vapor was generated, and then the heater wall temperature sharply decreased. Situation one in Table 2 lists the status variation of the working fluid during startup. According to the variation, three stages were determined: liquid heated (stage I), liquid superheated (stage II) and vapor generated (stage III). The criterion to determine stage I and stage II was based on the evaporation temperature. Since the evaporation temperature was obtained at a specific heat sink temperature, the demarcation for stage I and stage II was made with the evaporator outlet temperature equivalent to the evaporation temperature. Meanwhile, the criterion to determine stage II and stage III was based on the appearance of temperature decrease on heater wall, which meant the complete vaporization occurred. When the superheated liquid transformed to vapor, as shown in Figs. 7(a) and (b), sharp temperature spikes were found on the compensation chamber inlet and the compensation chamber outlet simultaneously. Owing to the large amount of transient vapor pressure generated in the vapor chamber, some vapor leaked through the gap to the compensation chamber. The fluid flowing through the compensation chamber was affected and heated. Subsequently, the compensation chamber inlet and outlet temperature stabilized, along with the cold liquid forced to the compensation chamber.

For the situation listed in Figs. 7(d)–(f), the loop was shut down for approximately 2 h before the heat load was applied to the evaporator. This situation was similar to that reported in our first loop [16]. Under these conditions, the vapor channels in the vapor chamber were partially occupied with liquid. Vapor remained in the vapor channels. After the liquid temperature reached the evaporation temperature, the remaining vapor served as effective nucleation sites for liquid boiling. Subsequently, after the evaporation condition was satisfied, the sensible heat and latent heat of the working fluid were used to dissipate the heat flux. The startup process between the heat load applied and the vapor generated was identical to that without any accumulated liquid. The differences

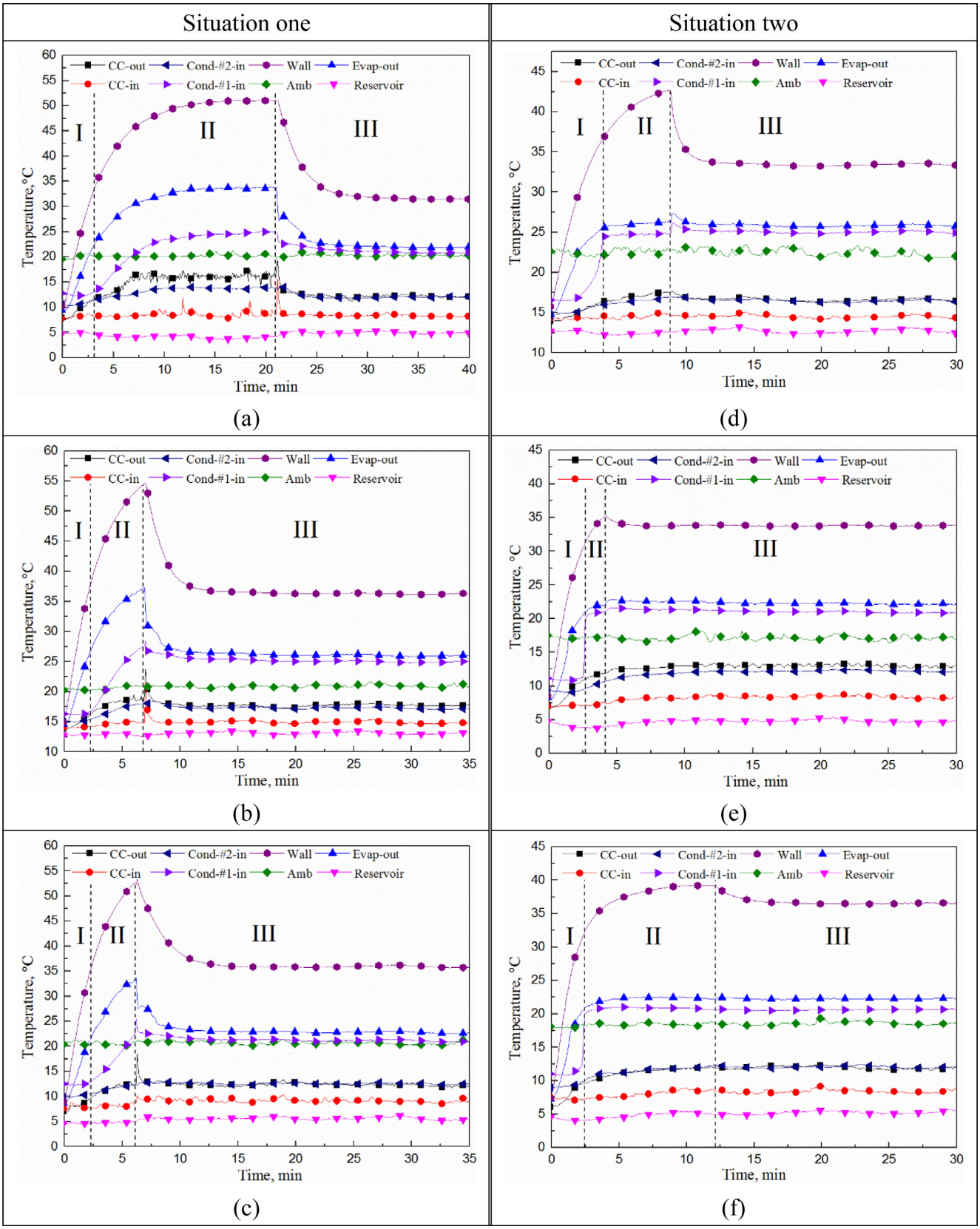

Fig. 7. Startup characteristics of the loop under different operational conditions: (a) Q = 50 W, P = 1.8 W, T_{sink} = 0 °C, (b) Q = 60 W, P = 2 W, T_{sink} = 10 °C, (c) Q = 70 W, P = 2 W, T_{sink} = 0 °C, (d) Q = 40 W, P = 2 W, T_{sink} = 10 °C, (e) Q = 60 W, P = 1.8 W, T_{sink} = 0 °C, (f) Q = 70 W, P = 2 W, T_{sink} = 0 °C.

occurred in the evaporation of the accumulated liquid. A sharp temperature decrease was found on the heater wall. Similarly, three stages were determined: liquid heated (stage I), thin-film boiling (stage II), and accumulated liquid vaporized (stage III). The criteria to determine stage I, stage II, and stage II were identical to that summarized in Figs. 7(a)–(c).

Table 2
Status variation of working fluid under different operational conditions.

Cases	Situation one	Situation two
Stage I	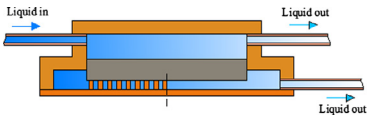	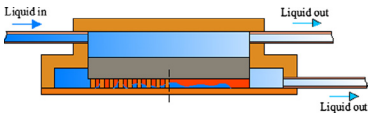
Stage II	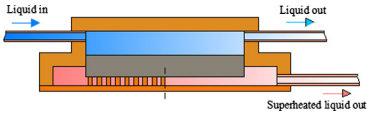	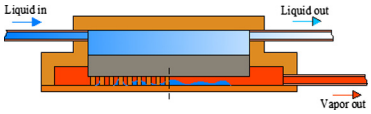
Stage III	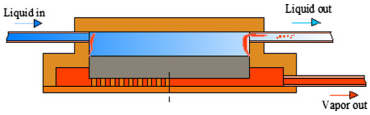	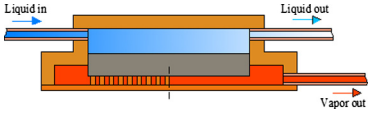

This study and our previous study showed an identical temperature overshoot on the heater wall. The difference between the present work and the previous wok was that the temperature overshoot of the heater wall during startup in this study could be classified into two types, while the previous work only showed one type. In this study, the loop experienced different time intervals, causing various initial liquid-vapor distributions in the evaporator. However, in our previous study, the loop operated in a continuous operation. The evaporator did not experience different initial liquid-vapor distributions. In summary, this study showed a comprehensive understanding of the impact of the initial liquid-vapor distribution on the startup characteristics of the pump-assisted capillary loop. Moreover, in this study, the accumulated liquid in the vapor channel vanished even though a low heat load was applied. Conversely, our previous study showed that the disappearance of the accumulated liquid only occurred at a high heat-load range. Owing to the decrease of the evaporation temperature in this study, the thin-film boiling mode replaced the flooding mode at low heat loads. Then, the accumulated liquid satisfied the evaporation condition more easily.

By comparing Figs. 7(a)–(c), the intervals for stages I, II, and III varied. This is shown in Figs. 7(d) –(f) as well. Meanwhile, the temperature overshoot was not equal at different operational conditions. The temperature overshoot ΔT_o was defined as:

$$\Delta T_o = T_p - T_s \tag{1}$$

Where T_p is the heater wall temperature value at the peak of the spike during startup, and T_s is the steady state operational temperature of the heater wall.

Table 3 concludes the time duration of the different stages and the temperature overshoot from Fig. 7. For situation one, as the heat load increased, the time durations for stages I and II gradually reduced. A higher heat load could accelerate the temperature increase of the working fluid in the evaporator. Hence, less time was spent for the transformations from the subcooled liquid to superheated liquid and superheated liquid to vapor. Meanwhile, it was determined that the value of the temperature overshoot dropped from 19.7 °C to 17.5 °C as the heat load increased from 50 W to 70 W. For situation two, the time duration of stage I for different heat loads accorded with the law that concluded in situation one. However, the time duration of stage II exhibited a random distribution. For situation two, as mentioned above, the vapor channels were partially occupied with liquid. For different time intervals before startup, the amount of accumulated liquid in the vapor channels was different. Meanwhile, the heat load and the heat sink temperature would change the rate of the temperature rise of the working fluid in the vapor chamber. As a result, under the influence of different heat loads, the accumulated liquid, and heat sink temperature, the time duration of stage II for situation two showed a random distribution. Moreover, the temperature overshoot was 9.3 °C, 1.7 °C, and 2.8 °C under the heat load of 40 W, 60 W, and 70 W, respectively.

3.2.3. Impact of the initial liquid-vapor distribution on the operational temperature

As shown in Figs. 8(a) and (b), the variable heat load test was performed. Before each test, the loop was shut down for approximately 2 h. Under this condition, the vapor channel was partially occupied with liquid. As shown in Fig. 8(a), the loop started at a low heat load of 20 W. As the loop reached a steady state, an identical temperature of the evaporator outlet and the condenser #1 inlet meant that vapor successfully generated and reached the condenser. Referring to the variation trend of the three stages, stage III did not appear at the heat load of 20 W. Eventually, the steady state temperature on the heater wall was 35 °C. Then, as the heat load increased to 70 W, the temperature overshoot appeared on the heater wall. Thus, stage III appeared at the heat load of 70 W, and the initial accumulated liquid vanished. Subsequently, the heat load returned to 20 W. The loop rapidly reached the equilibrium state, and the steady state temperature on the heater wall was 30 °C. Although the identical heat load of 20 W was applied to the evaporator, the loop exhibited a different operational temperature. A similar phenomenon appeared at the heat load of 30 W, as shown in Fig. 8(b). Difference during the operations with the heat load of 20 W was related to the difference of initial liquid-vapor distribution in the evaporator. The accumulated liquid in the vapor

Table 3
Time duration of different grades and the temperature overshoot ΔT_o.

Heat load, W	Situation one			Situation two		
	50.0	60.0	70.0	40.0	60.0	70.0
The time duration I, min	3.1	2.3	2.3	3.8	2.7	2.4
The time duration II, min	17.9	4.6	3.9	5.0	1.5	9.8
ΔT_o, °C	19.7	18.1	17.5	9.3	1.7	2.8

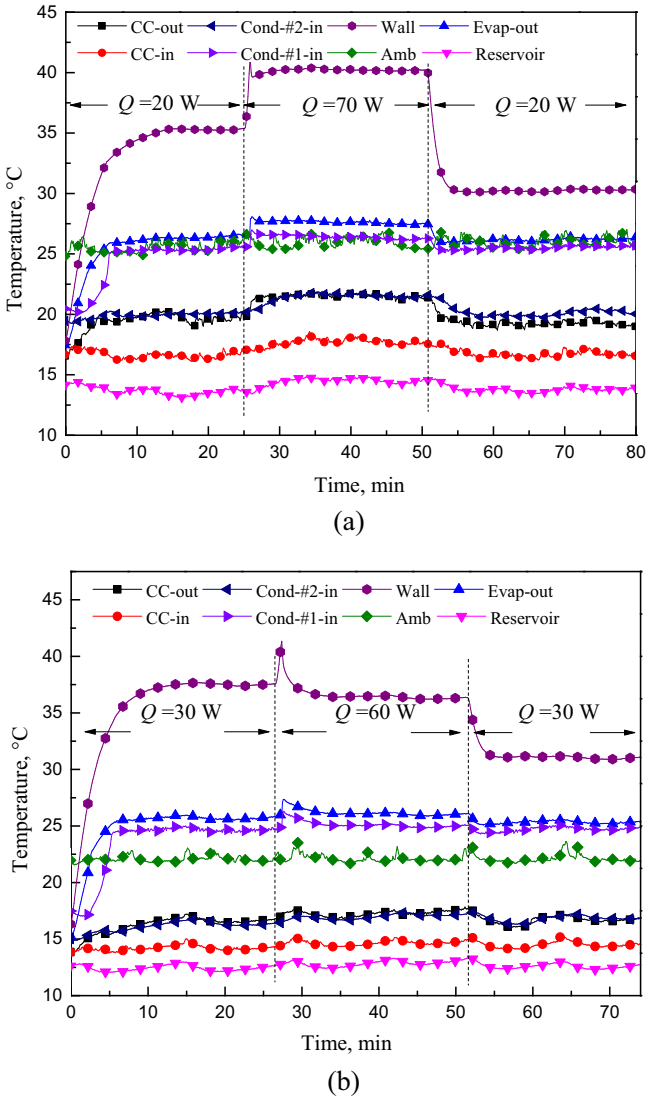

Fig. 8. Variable heat load test at the pumping power of 2 W and heat sink temperature of 10 °C.

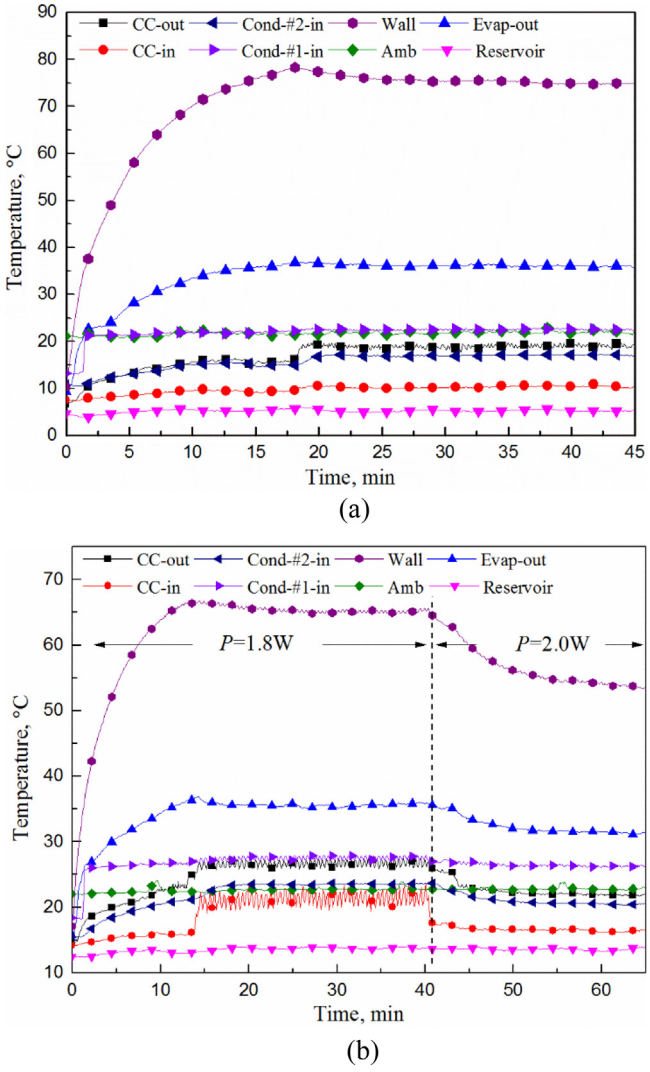

Fig. 9. Startup of the loop under high heat loads: (a) Q = 110 W, P = 2 W, T_{sink} = 0 °C, (b) Q = 90 W, T_{sink} = 10 °C.

channels blocked the vapor passages and increased the flow resistance of the vapor phase, thus resulting in a higher operational temperature. Therefore, owing to this adverse influence of the initial liquid-vapor distribution, we should take effective measures to eliminate the initial accumulated liquid in the vapor channels in the practical operation of the loop.

3.3. Effect of bubble generation in the compensation chamber

In an LHP operation, the temperature oscillation was associated with the thermal and hydrodynamic conditions in the compensation chamber [14]. The heat leak from the evaporator to the compensation chamber was the primary cause of the change of thermal and hydrodynamic conditions in the compensation chamber. Similarly, during the startup operation of the pump-assisted capillary loop, the heat leak affected the operational characteristics as well. Fig. 9 shows the startup characteristics of the loop under high heat loads. As illustrated in Fig. 9(a), the loop responded rapidly to the applied heat load. With a startup time of 1.5 min, the vapor was generated in the vapor chamber and then reached the condenser smoothly. Subsequently, the vapor in the vapor chamber gradually transformed to the superheated state. After the superheated vapor temperature at the evaporator outlet remained constant, at a start time of 18 min, a slight temperature increase of the compensation chamber outlet was observed. Simultaneously, the heater wall had a slight temperature drop. This indicated that the heat transfer capability of the evaporator contained an enhancement. As a higher heat load of 110 W was added to the evaporator, more heat leaked through the sidewall to the compensation chamber. Moreover, owing to the elevated vapor temperature (superheated vapor), the back-heat conduction through the porous wick to the compensation chamber also increased. Therefore, a phase change occurred, and a few vapor bubbles formed in the inner wall of the compensation chamber. Then, the heat transfer capability in the compensation chamber had an obvious enhancement, and a slight temperature drop appeared on the heater wall. Since liquid flowing through the compensation chamber was in the subcooled state, the generated vapor was removed by the liquid flow. Hence, the compensation chamber outlet temperature increased slightly. Subsequently, owing to the formation and removal of vapor bubbles in the compensation chamber, a small temperature fluctuation appeared on the profile of the compensation chamber outlet.

From Fig. 9(a), even though vapor bubbles were generated in the compensation chamber, the loop still had a stable operation. No obvious temperature oscillation was found on the heater wall. Therefore, the pump-assisted capillary loop performed better with vapor in the compensation chamber than the traditional capillary

loop. Fig. 9(b) shows another startup characteristic of the loop. With the startup pumping power of 1.8 W, a step temperature jump and temperature oscillation at the compensation chamber inlet and outlet appeared. The decreased subcooled liquid that returned to the compensation chamber owing to the elevated heat sink temperature of 10 °C weakened the cooling effect in the compensation chamber. Thus, the boiling in the compensation chamber became intense. After the pumping power increased from 1.8 to 2 W, the temperature oscillation disappeared on the compensation chamber inlet and outlet. This was because of the increased liquid flow rate through the compensation chamber, leading to the enhanced convective heat transfer in the compensation chamber. Then the vapor bubbles disappeared. According to the test result, once the vapor bubbles generated in the compensation chamber, increasing the liquid flow rate and lowering the heat sink temperature properly could prevent the boiling condition in the compensation chamber.

4. Conclusion

In this study, a comprehensive understanding on startup characteristics of the pump-assisted capillary phase change loop was obtained. The design of present loop was considered towards the practical application. To easily contact the heat source and effectively reduce the contact thermal resistance, a flat-type evaporator was designed. To create a lightweight loop, the impeller pump was adopted. The conclusions drawn from the experimental results were as follows:

(1) In this study, we proposed a reliable and efficient cooling loop that was confirmed to satisfy the heat dissipating demand of a high heat flux and a long transport distance.
(2) According to the startup characteristics of the loop under different operational conditions, this study revealed the three different modes: wick flooding, thin-film boiling, and vapor superheating. The three startup modes were validated as a general rule for the pump-assisted capillary phase change loop.
(3) As a pump-assisted capillary phase change loop was set up, the evaporation temperature of the working fluid depended mainly on the heat sink temperature, while changing the pumping power has nearly no impact on the evaporation temperature. Specifically, in this study, as the heat sink temperature lowered from 10 °C to -10 °C, the evaporation temperature dropped from 25 °C to 17 °C.
(4) This study revealed the impact of an initial liquid-vapor distribution on the startup characteristics of the pump-assisted capillary phase change loop. Different initial liquid-vapor distributions resulted in various temperature overshoots on the heater wall. Meanwhile, experimental results validated that the accumulated liquid in the vapor channel increased the resistance of vapor flow, thus resulting in the degradation of loop performance. Therefore, for the practical application of the pump-assisted capillary phase change loop, effective measures should be taken to eliminate the initial liquid impact on the operational characteristics.
(5) When the loop ran with a high heat load, the reliability of the pump-assisted capillary phase change loop was further validated. Even with a phase change of the working fluid in the compensation chamber, the loop could sustained a stable operation.

Acknowledgement

The present work was financially supported by the National Natural Science Foundation of China (No. 51276071).

Reference

[1] Y.F. Maydanik, Loop heat pipes, Appl. Therm. Eng. 25 (2005) 635–657.
[2] Y.F. Maydanik, M.A. Chernysheva, V.G. Pastukhov, Review: Loop heat pipes with flat evaporators, Appl. Therm. Eng. 67 (2014) 294–307.
[3] J. Li, F. Lin, D. Wang, W. Tian, A loop-heat-pipe heat sink with parallel condensers for high-power integrated LED chips, Appl. Therm. Eng. 56 (2013) 18–26.
[4] J. Li, L. Lv, Performance investigation of a compact loop heat pipe with parallel condensers, Exp. Therm. Fluid Sci. 62 (2015) 40–51.
[5] D.C. Mo, G.S. Zou, Y.Q. Wang, S.S. Lu, Flat loop heat pipe with bi-transport loops for graphics card cooling, Heat Transfer Eng. 35 (2014) 1071–1076.
[6] B.B. Chen, W. Liu, Z.C. Liu, H. Li, J.G. Yang, Experimental investigation of loop heat pipe with flat evaporator using biporous wick, Appl. Therm. Eng. 42 (2012) 34–40.
[7] B.B. Chen, Z.C. Liu, W. Liu, J.G. Yang, H. Li, D.D. Wang, Operational characteristics of two biporous wicks used in loop heat pipe with flat evaporator, Int. J. Heat Mass Transfer 55 (2012) 2204–2207.
[8] D.C. Mo, N. Ding, S.S. Lu, Gravity effects on the performance of a flat loop heat pipe, Microgravity Sci. Technol. 21 (2009) 95–102.
[9] X. Wang, J. Wei, Visual investigation on startup characteristics of a novel loop heat pipe, Appl. Therm. Eng. 105 (2016) 198–208.
[10] Y.F. Maydanik, V.G. Pastukhov, M.A. Chernysheva, Development and investigation of a miniature copper-acetone loop heat pipe with a flat evaporator, J. Electron. Cool. Therm. Control 05 (2015) 77–88.
[11] D. Wang, Z. Liu, J. Shen, C. Jiang, B. Chen, J. Yang, Z. Tu, W. Liu, Experimental study of the loop heat pipe with a flat disk-shaped evaporator, Exp. Therm. Fluid Sci. 57 (2014) 157–164.
[12] S. Wang, J. Huo, X. Zhang, Z. Lin, Experimental study on operating parameters of miniature loop heat pipe with flat evaporator, Appl. Therm. Eng. 40 (2012) 318–325.
[13] R. Singh, A. Akbarzadeh, M. Mochizuki, Operational characteristics of a miniature loop heat pipe with flat evaporator, Int. J. Therm. Sci. 47 (2008) 1504–1515.
[14] D. Gai, W. Liu, Z. Liu, J. Yang, Temperature oscillation of mLHP with flat evaporator, Heat Transfer Res. 40 (2009) 321–332.
[15] X. Zhang, J. Huo, S. Wang, Experimental investigation on temperature oscillation in a miniature loop heat pipe with flat evaporator, Exp. Therm. Fluid Sci. 37 (2012) 29–36.
[16] C. Jiang, W. Liu, H.C. Wang, D.D. Wang, J.G. Yang, J.Y. Li, Z.C. Liu, Experimental investigation of pump-assisted capillary phase change loop, Appl. Therm. Eng. 71 (2014) 581–588.
[17] C. Park, M. Crepinsek, Effect of operational conditions on cooling performance of pump-assisted and capillary-driven two-phase loop, J. Thermophys. Heat Transfer 25 (2011) 572–580.
[18] M. Crepinsek, C. Park, Experimental analysis of pump-assisted and capillary-driven dual-evaporators two-phase cooling loop, Appl. Therm. Eng. 38 (2012) 133–142.
[19] C. Park, A. Vallury, J. Zuo, Performance evaluation of a pump-assisted, capillary two-phase cooling loop, J. Therm. Sci. Eng. Appl. 1 (2009) 022004.
[20] B.R. Babin, G.P. Peterson, J. Seyed-Yagoobi, Experimental investigation of an ion-drag pump-assisted capillary loop, J. Thermophys. Heat Transfer 7 (1993) 340–345.
[21] N. Schweizer, P. Stephan, R. Schlitt, A concept for a miniature mechanically pumped two-phase cooling loop, SAE Technical Paper, 2008-01-1953, 2008.
[22] T.T. Hoang, R.W. Baldauff, R.W. Baldauff, Hybrid two-phase mechanical capillary pumped loop for high-capacity heat transport, SAE Technical Paper, 2007-01-3198, 2007.
[23] J. Liu, M. Lv, S. Zhang, K. Guo, Z. He, T. Li, Experimental investigation on start-up of mechanically pumped cooling loop, Energy Convers. Manage. 49 (2008) 2595–2601.
[24] H. Zhang, G. Lin, T. Ding, W. Yao, X. Shao, R.G. Sudakov, Y.F. Maidanik, Investigation on startup behaviors of a loop heat pipe, J. Thermophys. Heat Transfer 19 (2005) 509–518.
[25] S. Wang, W. Zhang, X. Zhang, J. Chen, Study on start-up characteristics of loop heat pipe under low-power, Int. J. Heat Mass Transfer 54 (2011) 1002–1007.
[26] J.H. Boo, E.G. Jung, Bypass line assisted start-up of a loop heat pipe with a flat evaporator, J. Mech. Sci. Technol. 23 (2010) 1613–1619.
[27] W. Joung, K. Gam, K. Park, S. Ma, J. Lee, Transient responses of the flat evaporator loop heat pipe, Int. J. Heat Mass Transfer 57 (2013) 131–141.
[28] L. Bai, G. Lin, D. Wen, Modeling and analysis of startup of a loop heat pipe, Appl. Therm. Eng. 30 (2010) 2778–2787.
[29] L. Bai, G. Lin, D. Wen, J. Feng, Experimental investigation of startup behaviors of a dual compensation chamber loop heat pipe with insufficient fluid inventory, Appl. Therm. Eng. 29 (2009) 1447–1456.
[30] B. Duan, M. Luo, C. Yuan, X. Luo, Multi-objective hydraulic optimization and analysis in a minipump, Sci. Bull. 60 (2015) 1517–1526.
[31] C. Jiang, Z. Liu, D. Wang, J. Yang, H. Wang, J. Li, W. Liu, Effect of liquid charging process on the operational characteristics of pump-assisted capillary phase change loop, Appl. Therm. Eng. 91 (2015) 953–962.